

Modification of MWCNT and Its Effect on ABS/LCP Blend System

Goutam Hatui,¹ Ganesh Chandra Nayak,¹ Chapal Kumar Das,¹ Samar B. Yadaw²

¹Materials Science Centre, Indian Institute of Technology, Kharagpur 721302, India

²Defence Materials and Stores Research Development and Establishment, Kanpur 208013, India

Correspondence to: C. K. Das (E-mail: chapal12@yahoo.co.in)

ABSTRACT: Multiwalled carbon nanotubes (MWCNTs)/acrylonitrile-butadiene-styrene (ABS) composites with unmodified and modified (COOH-MWCNTs) CNTs were prepared using the melt blending method. The composites with 0, 1, and 1.5 phr MWCNTs (with and without modification) were analyzed by scanning electron microscopy and transmission electron microscopy, and better dispersion was observed for the acid-modified MWCNTs. In addition, a network structure was observed for the modified MWCNTs added system. The mechanical and electrical properties of the composite with different parts per hundred of nanotubes were increased, but the effect was pronounced with modified MWCNTs due to the better interaction of modified MWCNTs with the polymer matrices. The thermal stability of the composites was also strongly improved with MWCNTs loading. Blending of liquid crystalline polymer (LCP, Vectra A950) with ABS/MWCNTs resulted in further improvement in electrical and thermal properties. This improvement can be ascribed to the self-reinforcing tendency of LCPs (due to their rigid rod-like molecular structure), which act as a load-bearing agent in the blend matrix. The possible interaction between –CN group of ABS and ester group of LCP with the –COOH group of modified MWCNTs enhanced the interfacial adhesion between ABS and LCP. © 2012 Wiley Periodicals, Inc. *J. Appl. Polym. Sci.* 129: 57–64, 2013

KEYWORDS: adhesives; blends; compatibilization; liquid crystals; morphology

Received 21 July 2012; accepted 2 October 2012; published online 3 November 2012

DOI: 10.1002/app.38684

INTRODUCTION

In recent years, there has been intense interest in multiphase polymer blends due to the potential opportunities of combining the attractive features of each blend component while at the same time reducing their deficient characteristics.^{1,2} However, binary blends of immiscible polymers generally exhibit poor mechanical properties due to a coarse and often unstable morphology, such as in polypropylene/polyamide blends.³ Therefore, it is essential to control and stabilize a desired type of morphology in a polymer blend in order to generate polymeric materials with favorable properties.

Recently, carbon nanotubes (CNTs) have been described as effective conducting filler for polymers. Nanotubes can be described as long and slender fullerenes, in which the walls of the tubes are hexagonal carbon (graphite structure). These tubes can either be single-walled or multiwalled CNTs (MWCNTs). Kara et al. has shown that the insulator–conductor transition takes place by addition of a small amount of MWCNT in the PS–MWCNT composite system. The CNTs also have excellent electrical properties; in theory, metallic CNTs can have electrical conductivities more than 1000 times greater than metals such as copper.⁴ Using MWCNTs, and taking into account the defects

in CNTs, the electrical conductivities are lower by one or two orders of magnitude, which still means they have outstanding electrical conductivities. The electrical percolation threshold of composites depends on what kind of CNTs are used, the preparation method of the CNTs, the matrix polymer, and especially the dispersion of the CNTs. We have also seen^{5,6} that the percolation threshold varies exponentially with the aspect ratio, which implies that, for discernible mechanical property differences, large aspect ratio changes would be needed. For these reasons, an exact percolation threshold cannot be given for CNTs, although the electrical percolation threshold is usually about 0.1–3 wt % CNTs.⁷ It was found that optical percolation process for polymer–CNT thin film composites could also be observed by using optical transmission technique.⁸ Thorstenson et al. have described the use of nanotubes to produce composite materials with superior electrical properties.⁹ Although CNTs–polymer composites hold great promise, the dispersion of CNTs and the weak interface between the nanotubes and the polymer matrix are issues critical to successful applications. For the better interfacial adhesion and good dispersion of CNT in polymer matrix, chemical treatments such as acid oxidation and free radical reaction are the most often methods that have been conducted.^{10–12} The attachment of functional groups to the

surface of nanotubes can improve the efficiency of load transfer. However, it must be noted that these functional groups might introduce defects on the walls of the perfect structure of the nanotubes. These defects will lower the strength of the reinforcing component. Therefore, there will be a trade-off between the strength of the interface and the strength of the nanotubes filler.

Meincke et al. has shown that the nanotubes cause a significant increase in stiffness, but, on the other hand, this material shows a brittle behavior indicated by the low elongation at break in the tensile test.¹³ The dispersion of MWCNTs, in the polymer matrix, is affected by the processing conditions. The influence of processing conditions on the state of dispersion of MWCNTs in polymeric matrices has been described by Potschke and Bhattacharaya.¹⁴ They have shown that the nanotubes dispersed uniformly throughout the matrix by compounding a polycarbonate master batch with the corresponding neat polymer in a twin-screw compounder. No signs of segregation or depletion of MWCNTs at the surface of extruded samples was found. The major drawback of MWCNTs is the agglomeration tendency, due to the van der Waals force of attraction between the nanotubes, due to which it is very difficult to disperse them in the polymer matrices. This issue can be addressed by the chemical modification of MWCNTs, which can enhance the interaction with the polymer matrix and in turn better dispersion can be achieved. Functionalization of CNTs not only improves their dispersion but also enhances the adhesion at the nanotube–polymer interface via specific interaction like hydrogen bonding between the surface functional group of CNT and the polar groups of polymer.

The MWCNTs can affect the properties of polymer blends in a number of ways. First, the stability of the cocontinuous morphology should be improved by the addition of a reactive compatibilizer and the filler, if one manages to confine the filler to only one phase of the blend. Second, in this case, electrical conductivity should be observed at rather small loadings of nanotubes in the blend due to a double percolation phenomenon.¹⁵ Third, due to the high stiffness of nanotubes, the mechanical properties should be enhanced substantially.¹⁶ Needleman et al. have shown that analyzed the tensile response of an idealized CNT-reinforced polymer composite and explored the effects of the interphase on reinforcement debonding and results reveal the significant role that an interphase can play in determining the overall stress carrying capacity of the CNT-reinforced composite and how internal stresses are redistributed when fiber debonding takes place.¹⁷ Nayak et al.¹⁸ have shown pure and SiC-modified MWCNTs are dispersed in the PPO/liquid crystalline polymer (LCP) blend by melt mixing. SiC coating improves the dispersion of modified MWCNTs compared to pure MWCNTs. This improved dispersion results in enhanced thermal stability of the S-MWCNTs added nanocomposites compared to pure MWCNTs. This improved dispersion results in enhanced thermal stability of the S-MWCNTs added nanocomposites compared to pure MWCNTs. Viscosity as well as storage modulus enhancement of PES/LCP/CNT blend signifies better interfacial adhesion exists in the above-mentioned blend systems as compared to PES/LCP blend.¹⁶

The present study focused on the evaluation of effect of surface functionalization of CNTs, on the properties of acrylonitrile-

butadiene-styrene (ABS) and ABS/LCP blend system with special attention on the dispersion and phase adhesion. The pristine MWCNTs were acid modified to improve the dispersion in the polymer matrix and to improve the interaction with the blend matrix. The phase adhesion between ABS and LCP by the functionalized CNT is discussed. The percolation of CNTs is described, based on measurements of electrical conductivity.

EXPERIMENTAL

Materials Used

The ABS resin (GPM 5500) was purchased from GE Plastics, India. The molecular weight of the resin is 2.5×10^4 g/mol, the density is 1.04 g/cm^3 , and the melt flow rate is 7.0 g/10 min at 220°C at the load 5 kg . ABS resin consists of a styrene-acrylonitrile copolymer matrix and a styrene-butadiene copolymer dispersed rubber phase. The LCP was Vectra A950, purchased from Ticona (Shelby, NC). Its density is 1.4 g/cm^3 . This LCP is wholly aromatic copolyester consisting of $25 \text{ mol } \%$ of 2,6-hydroxynaphthoic acid and $75 \text{ mol } \%$ of *p*-hydroxybenzoic acid. The molecular weight could not be determined because it was difficult to find a suitable solvent in which it could be dissolved. The MWCNTs (MWCNTs-1000) were from IJin Nano Technology, Korea. CNTs were used with and without modification. The diameter, length, and aspect ratio were $10\text{--}20 \text{ nm}$, $20 \mu\text{m}$, and ~ 1000 , respectively. The density of MWCNTs was 2.16 g/cm^3 .

Preparation of Functionalized MWCNTs

Briefly, pure MWCNTs (500 mg) were first ultrasonicated in tetrahydrofuran for 8 h at 60°C and then refluxed at 120°C for 4 h using a round-bottom conical flask with a magnetic stirrer (mild stirring). After cooling, the mixture was washed with distilled water. A $3 : 1$ concentrated $\text{H}_2\text{SO}_4/\text{HNO}_3$ mixture is commonly used for modification because it can intercalate and exfoliate graphite layers.^{19,20} It etches away the ends and a side-wall defect sites, where ring strain is large enough to allow chemical attack and incorporate carboxylic acid groups. In other words, it will open the ends and convert the capped CNTs into open fullerene pipes. The radicals at the ends were stabilized by bonding with carboxylic acid ($-\text{COOH}$) or hydroxylic ($-\text{OH}$) groups. So, by this process, COOH-MWCNT will be formed.

Preparation of Nanocomposites

Before mixing, the ABS and LCP (Vectra A950) pellets were dried inside a vacuum oven at 70°C for 4 h and 120°C for 8 h , respectively. MWCNTs-1000 were dried under vacuum at 300°C for 4 h . ABS/MWCNTs composites containing pure MWCNTs [$1.5 \text{ parts per hundred (phr)}$] and modified COOH-MWCNTs (1.5 phr) were melt blended in a twin-screw extruder, which was equipped with a screw of 19 mm in diameter, compression ratio ($3 : 1$), and L/D (length/diameter) ratio of 25 . The extrusion temperatures of the feeding zone/transporting zone/melting zone were set at $160^\circ\text{C}/250^\circ\text{C}/280^\circ\text{C}$ at 60 rpm . It is a counter rotating twin-screw extruder, and the mixing is occurring in between the two screws and in between the screw and the wall because of high shear stress and shear rate encountered in these two zones. There are no extra mixing zones. Length/diameter ratio ($=25$) is sufficient for mixing the two thermoplastics as reported by Bose et al.²¹ The LCP (15 phr content) was added to ABS/ COOH-MWCNTs (1.5 phr) blend. The ABS/ COOH-

Table I. Showing the Composition of the Samples

Sample code	ABS (phr)	MWCNTs (phr)	COOH-MWCNTs (phr)	ABS/COOH-MWCNTs/LCP (phr)
A	100	-	-	-
B	100	1	-	-
C	100	1.5	-	-
M	100	-	1.5	-
D	85	-	1.5	15

MWCNTs/LCP blends were also extruded with same temperature profile. The extrudates were also pelletized. Dog bone-shaped tensile bars were compression molded. Blending formulation is given in Table I.

Characterizations

Infrared Measurement. Fourier transformation infrared (FTIR) spectroscopy was recorded on a NEXUS 870 FTIR (Thermo Nicolet) instrument to detect the functional group incorporated on the surface of MWCNT after acid modification. The tests were conducted in a moisture-free atmosphere at room temperature from 400 to 4000 cm^{-1} .

Differential Scanning Calorimetry Study. Differential scanning calorimetry (DSC) was performed under a nitrogen flow (40 mL/min) using a NETZSCH DSC 200PC instrument. The samples (6.5 mg) sealed under aluminum pans were scanned in the temperature range of room temperature to 350°C at 10°C/min.

Dynamic Mechanical Analysis. Dynamic mechanical properties of the composites were analyzed using a TA instrument (DMA 2980 unit) in single cantilever bending mode. The samples were subjected to a frequency of 1 Hz from 50°C to 250°C and a heating rate 10°C/min.²²

Field-Emission Scanning Electron Microscopy Study. Field-emission scanning electron microscopy (FESEM) analysis was done using a JEOL ISM-5800 (Carl Zeiss- SUPRA™ 40). The cryofractured surfaces were coated with a thin layer of gold (5 nm). During scanning of the composites, the pressure of the vacuum was in the order of 10⁻⁴–10⁻⁶ mmHg.

Mechanical Testing. Dumb bell-shaped testing samples were used for tensile testing. After moulding, samples were kept for 24 h to relax the stresses induced during cooling. Mechanical properties were measured using a Hounsfield HS 10 KS (universal testing machine), at room temperature with a crosshead speed of 5 mm/min and an initial gauge length of 35 mm and with a load cell of 10 kN according to ASTM D638 as reported by Hatui et al.²³ The results reported are the averages of four samples for each composite.

Conductivity Measurements. The electrical resistivity was measured on a compression-molded square slab (sides 1 cm, thickness 3 mm). A Keithley 230 Programmable voltage source test fixture was used to measure volume resistance. Pressed samples were put into two probe conductivity apparatus. Using eq. (1), the resistivity, ρ , was calculated. In present work, the electrical resistivity has been calculated by taking into considera-

tion the dispersion of MWCNTs throughout the volume of matrix. Electrical resistivity is an absolute value specific to the material. Electrical resistivity is also useful for evaluating the relative dispersion state of a conductive additive throughout the polymer matrix:

$$\rho = R_{ot}/L. \quad (1)$$

Transmission Electron Microscopy. The extent of dispersion of MWCNT in the polymer matrix is studied by transmission electron microscopy (TEM; FEI™, Type 5022/22, Technai G2 20 S-Twin) operating in an accelerating voltage of 80 kV. Composites are ultramicrotome under cryogenic condition with a thickness of around 50–80 nm.

RESULTS AND DISCUSSION

Functionalization of CNTs

The surface functionalization of MWCNTs was confirmed by FTIR. The FTIR spectra of functionalized MWCNTs and pure MWCNTs are shown in Figure 1. For the pure MWCNTs, a weak peak was observed at about 3498 cm^{-1} , due to the presence of hydroxyl groups (–OH) on the surface of the MWCNTs, which were believed to result from oxidation during purification of the raw material.²⁴ For the acid-modified MWCNTs, FTIR spectra showed new peaks in comparison to pure MWCNTs. New bands appeared at 3492 cm^{-1} due to the presence of –OH and –COOH groups on MWCNT surface. In addition, new peaks at 1721 cm^{-1} [ascribed to the characteristic peak of acidic carbonyl (C=O) stretching] and around 1565 cm^{-1} (vibrational mode of carbon skeleton of CNTs) were observed.

Thermomechanical Properties and DSC Analysis of Composites

The effect of functionalization of MWCNTs on the thermomechanical properties of ABS and ABS/LCP blend system was analyzed by dynamic mechanical thermal analysis (DMTA). Figure 2(a,b) shows the storage modulus and $\tan \delta$ of plots of different composites, respectively. Storage modulus of ABS increased with the incorporation of 1 and 1.5 wt % of MWCNTs; however, the increase is prominent with acid-modified MWCNTs. The modulus achieved with the incorporation of

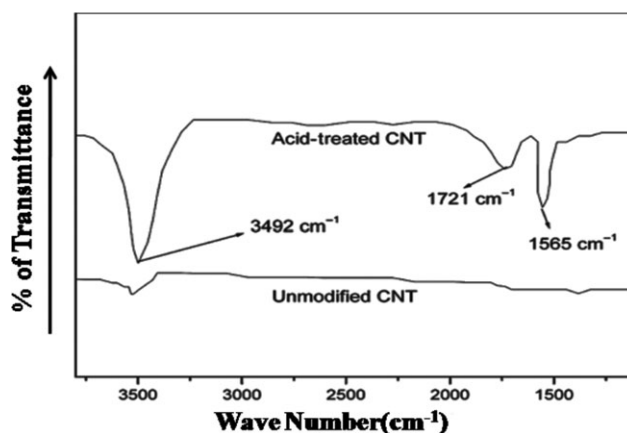


Figure 1. Showing FTIR spectra of pure and modified MWCNTs.

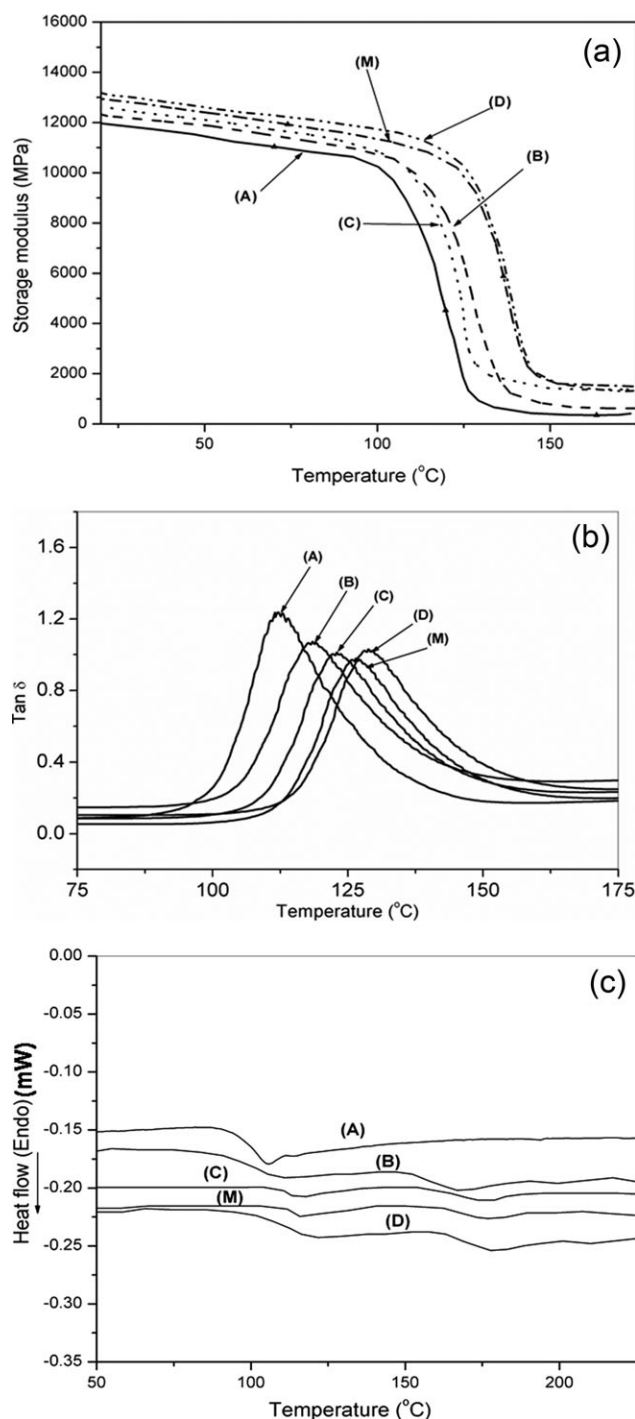


Figure 2. (a) Dynamic mechanical analysis: storage modulus (E'), (b) Damping factor for ABS/MWCNTs and ABS/MWCNTs/LCP composite. (c) DSC curves showing glass transition temperature of ABS/MWCNTs and ABS/MWCNTs/LCP composite.

1.5 wt % of acid-modified MWCNTs was found to be higher than that of 1.5 wt % unmodified MWCNT added to ABS nanocomposite. This enhancement in the storage modulus, for the modified MWCNTs system, can be ascribed to two factors. First, the agglomeration tendency of unmodified MWCNTs restricts the reinforcing effect due to the lack of access to all the

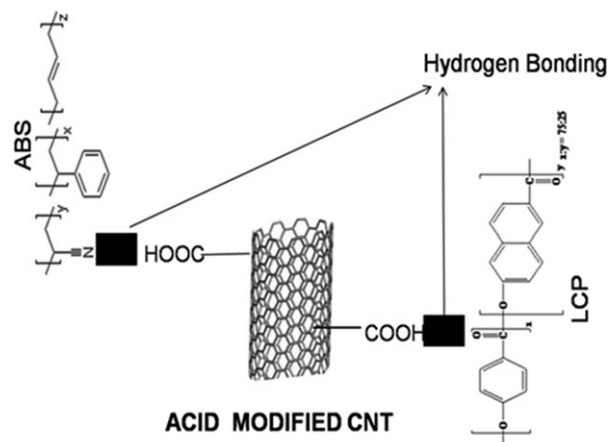


Figure 3. Showing the bridging effect of modified MWCNT.

nanotubes by the ABS matrix. Second, the load transfer to the nanotubes will only be effective if there is a strong interaction at the nanotube–polymer interface, which was achieved for the modified MWCNTs via interactions between the $-COOH$ of CNTs and $-C\equiv N$ of ABS. The better adhesion of ABS matrix with the modified MWCNTs enhanced the effective load transfer to the nanotubes as compared to unmodified MWCNTs, which increased the storage modulus. In case of ABS/LCP blend nanocomposite, the increase in the storage was found to be superior among all the systems studied. In our previous work with ABS/LCP/MWCNTs, we have showed that blending of ABS/LCP resulted in an incompatible polymer blend where the modulus showed marginal change.²⁵ We have predicted that the incompatibility between the ABS and LCP can be addressed with the modified MWCNTs, due to their high aspect ratios, which can bind the blend partners together. A schematic diagram of this interaction is shown in Figure 3. This improvement in phase adhesion, between ABS and LCP, can enhance the load transfer from ABS to LCP and to the modified MWCNTs, which can increase the storage modulus. This has been discussed in detail in the following section.

Figure 2(b) shows the $\tan \delta$ plots and the respective properties are summarized in Table II. Incorporation of MWCNTs decreased the $\tan \delta$ peak heights and hence improved the damping nature of composites as compared to neat ABS. This phenomenon can be attributed to (i) the better adhesion between ABS and acid-treated MWCNTs (hydrogen bonding

Table II. Showing the Glass Transition Temperature and $\tan \delta$ of the Composites

Sample code	T_g ($^{\circ}C$) from DMTA	T_g ($^{\circ}C$) from DSC	$\tan \delta$ (maximum)
A	112 ± 1	109 ± 1	1.21 ± 0.03
B	118 ± 2	111 ± 2	1.10 ± 0.02
C	122 ± 1	114 ± 1	1.00 ± 0.03
M	125 ± 1	116 ± 1	0.90 ± 0.04
D	128 ± 1	120 ± 2	1.05 ± 0.03

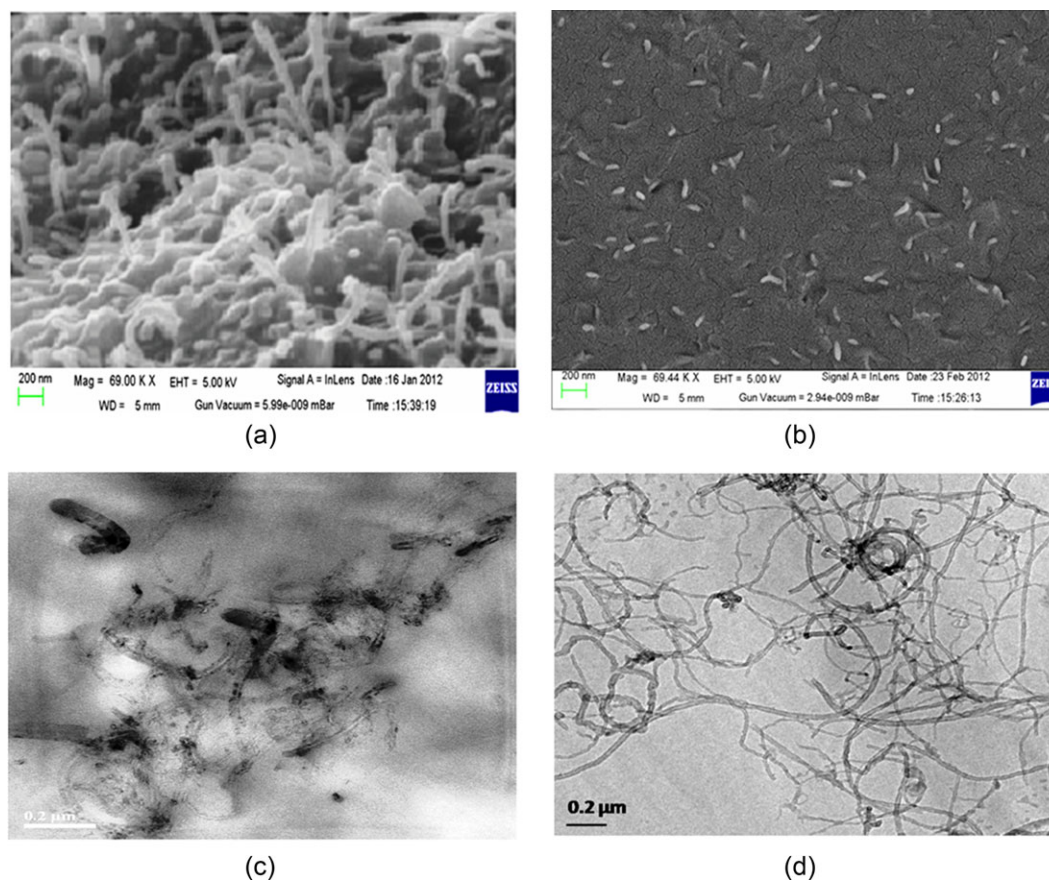


Figure 4. (a) Showing FESEM images of the fracture surface in composites containing 1 phr of untreated MWCNTs/ABS composites. (b) Showing FESEM images of the fracture surface in composites containing 1.5 phr of acid-treated MWCNTs/ABS composites. (c) TEM image showing the agglomeration of MWCNT in ABS/unmodified MWCNT system. (d) Showing the dispersion of modified MWCNT in ABS/modified MWCNT system. [Color figure can be viewed in the online issue, which is available at wileyonlinelibrary.com.]

between modified CNT and ABS-LCP, Figure 3), which effectively restricts the movement of molecular chains and allows better stress transfer from matrix to CNTs permitting only a small part of it to strain the interface. Hence, the strong interface is characterized by less energy dissipation.²⁵ (ii) Heat build-up is minimized in the nanocomposites, which favors the improved damping properties.

From Table II, it is clear that addition of MWCNTs increased the glass transition temperature (T_g) as compared to pure ABS (109°C).²⁶ Composites containing the acid-treated MWCNTs (D and M) showed highest glass transition temperature. This can be due to the hydrogen bonding interaction between the polar $-CN$ group of ABS and hydrogen of $-COOH$ of MWCNTs. This hydrogen bonding restricted the segmental motion of the ABS chains in the vicinity of MWCNTs and hence increased the T_g . In case of LCP-added composite (D), the acid-treated MWCNT acts as a bridging agent (Figure 3) at the interface of ABS and LCP and hence impart rigidity to the system due to which an increase T_g was observed.²⁷

The T_g of different system was also measured by DSC and shown in Figure 2(c). The respective parameters are shown in Table II. DSC analysis also showed the same trend of T_g as that

of DMTA but showed different values compared to DMTA analysis. This is because of the differences in the measured techniques: DMTA is dynamic process whereas DSC is static process.

Field-Emission Scanning Electron Microscope

After conducting tensile tests of the ABS/MWCNTs composites, the fracture surfaces were observed by FESEM to investigate the dispersion and adhesion state of MWCNTs in the matrix phase. The untreated MWCNTs dispersed as agglomerates in the polymer matrix, whereas the acid-treated MWCNTs were dispersed uniformly in ABS matrix, as shown in Figure 4(a,b).

This better dispersion can be attributed to the enhanced interaction between the modified MWCNTs and ABS matrix, which increased the wetting of MWCNTs, by ABS matrix, after modification. The interaction between $-COOH$ group of modified MWCNTs and $-C=N$ group of ABS increased the adhesion at the nanotube-polymer interface and resulted in better stress transfer to the nanotubes. The interaction between the modified MWCNTs and ABS matrix through the hydrogen bonding interaction (Figure 3) was relatively strong, as compared to the physical interaction between the untreated MWCNTs and ABS. These kinds of interactions results in an effective stress transfer

Table III. Mechanical Properties of the ABS, ABS/MWCNTs, and ABS/MWCNTs/LCP Composite

Sample code	A	B	C	M	D
Tensile strength (MPa)	45.8 ± 1.8	51.2 ± 1.9	56.4 ± 2.1	64.6 ± 1.5	68.9 ± 1.8
Young's modulus (GPa)	2.37 ± 0.1	3.1 ± 0.2	3.9 ± 0.1	4.6 ± 0.1	4.9 ± 0.2
Elongation at break (%)	26.5 ± .2	22.4 ± .1	12.1 ± .2	11.5 ± .3	11.3 ± .2

from matrix to MWCNTs and thus a high tensile strength for the composite (discussed in the Mechanical Properties section).

To further confirm the better dispersion, TEM analysis was carried out and the images are presented in Figure 4(c,d). As can be seen, unmodified MWCNTs were agglomerated in the ABS matrix whereas modified MWCNTs were better dispersed in the polymer matrix. This observation supports the FESEM analysis where acid-modified MWCNTs well dispersed in the ABS matrix.

Mechanical Properties

The mechanical properties of composites depend on many factors, including the aspect ratio of the filler, degree of dispersion, and the adhesion at the filler–matrix interface. Table III demonstrates the tensile strength, elongation at break, and Young's modulus of the ABS/MWCNTs composite. The prime aim of functionalization of CNTs is to achieve better dispersion and interaction in and with the matrix to control the properties of CNT-reinforced polymer nanocomposite. The functionalization can be achieved by noncovalent and covalent bonding of functional groups upon the CNTs. However, for a noncovalent modification, there could be interfacial slippage at the CNT–functional group interface. That means if the interaction of functional group with the matrix is stronger than that with the CNT, then the nanotubes will be dragged out of the matrix during mechanical testing and resulted in the failure of the nanocomposite. However, if the functionalization is a covalent one, then the slippage at the CNT–functional group interface can be avoided and drag out of CNTs during mechanical testing can be avoided, which will enhance the mechanical properties. That is why, we did the covalent modification of CNTs. In comparison to the pure ABS, composites containing MWCNTs (with and without modification) showed higher tensile strength and modulus, and the increase was pronounced in ABS/acid-modified MWCNTs composites.

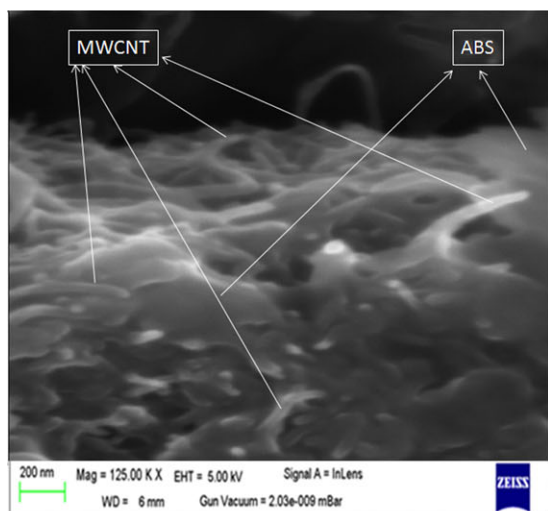
The improvement in tensile strength and modulus of ABS/MWCNTs–COOH (1.5 wt %) was due to the strong interactions between ABS matrix and MWCNTs–COOH. As the functionalized MWCNTs prepared by acid treatment contain –COOH groups, these were helpful for improving the interaction between CNTs and ABS matrix. Therefore, the strong interaction between the functionalized MWCNTs and the ABS matrix greatly enhanced the dispersion quality as well as the interfacial adhesion, thus enhanced the overall mechanical performance of the composite. The elongation-at-break of samples was lower in presence of MWCNTs, which showed that the inclusion of MWCNTs made the ABS stronger but more brittle too. The incorporation of modified MWCNT to the polymer matrix leads to decrease in the elongation at break. This is mainly due

to increased stiffness of polymer matrix upon addition of nanofillers (here MWCNTs). This decrease in elongation at break upon addition of nanofillers to the polymer matrix has already been mentioned in various literatures.¹⁸

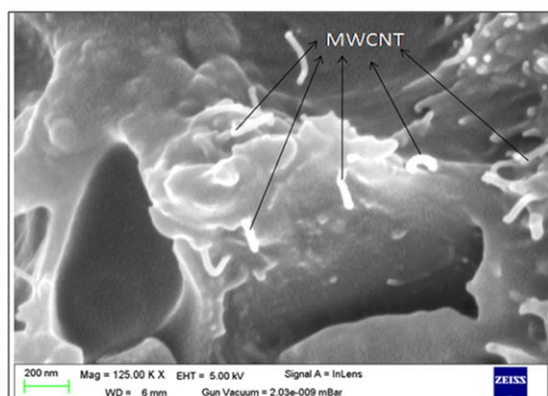
Tensile strength and modulus showed an upward trend for the addition of unmodified and modified MWCNTs to the ABS matrix. Incorporation of acid-modified MWCNTs to the ABS/LCP blend system increased the tensile strength and modulus significantly as compared to pure ABS and other nanocomposites. In our previous work also, we had only achieved 51 MPa and 2 GPa as tensile strength and modulus, respectively, for the ABS/LCP blend system, which was due to the incompatibility between the blend partners.²⁵ But, incorporation of acid-modified MWCNT increases the phase adhesion between the blend partners, which increase the tensile properties significantly. To clarify this, FESEM images were taken at low and high magnifications and presented in Figure 5(a–c). Figure 5(a) shows the agglomeration of unmodified MWCNTs in the ABS matrix. In contrast to this, a better dispersion was observed for the acid-modified MWCNTs added to ABS nanocomposite [Figure 5(b)]. Interestingly, for ABS/LCP/modified MWCNTs, the nanotubes were found to be holding the two polymer phases intact. As can be seen from Figure 5(c), the nanotubes were bridging the LCP phase with the ABS, which not only improved the adhesion between the ABS and LCP but also enhanced the load transfer from ABS to rigid LCP. This better adhesion and load transfer increased the strength and modulus of the ABS/LCP blend system. This is in well accordance with the storage modulus data, where a superior property was observed for the ABS/LCP blend nanocomposite.

Electrical Resistivity

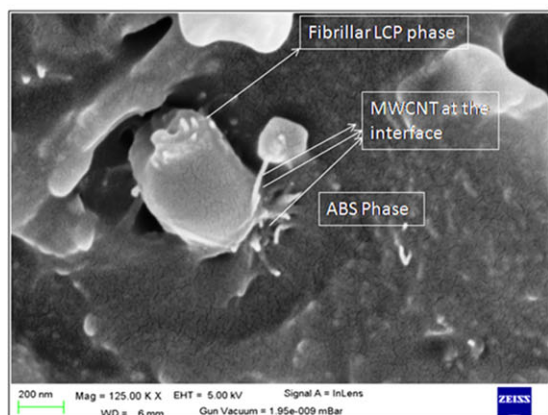
Volume electrical resistivity of the composites was measured with two probe conductivity apparatus. The results are summarized in Figure 6. ABS is an excellent insulating material with volume electrical resistivity of about $10^{15} \Omega \text{ cm}$, while CNTs have electrical characteristics that were similar to metallic/semi-metallic materials; therefore, the addition of MWCNTs into the polymer improves its electrical conductivity. The dispersed MWCNTs form conducting channels within the isolating polymer matrix, which enhances the ability of the composite films to conduct charge. Due to the formation of percolating network by MWCNTs in the polymer, the minimum amount of nanotubes required for a conducting network spanning the polymer matrix depends on the degree of debundling and dispersion of the nanotubes. In the present work, the influence of CNTs on the room temperature resistivity of ABS/MWCNTs composite containing 1 phr (pure MWCNTs) and 1.5 phr (pure and modified MWCNTs) was investigated. The resistivity reduced from



(a)



(b)



(c)

Figure 5. (a) Higher magnification of FESEM image showing agglomerated MWCNT in ABS matrix. (b) Higher magnification of FESEM image showing better dispersion of acid-modified MWCNT in ABS. (c) Higher magnification of FESEM image showing bridging effect of MWCNT at the interface of ABS and LCP. [Color figure can be viewed in the online issue, which is available at wileyonlinelibrary.com.]

10^{15} to $2.51 \times 10^{13} \Omega \text{ cm}$ at 1 phr of pure MWCNTs. A significant drop in resistivity of the composite films was observed at MWCNTs loading of 1.5 phr from 2.1×10^{15} to $7.0 \times 10^7 \Omega$

cm, which was about 7 orders of magnitude decrease as compared to pure ABS.

However, with the addition of modified MWCNTs (1.5 phr), the composite displayed a further decrease in resistivity ($1.9 \times 10^6 \Omega \text{ cm}$). This indicates improved dispersion and formation of higher number of interconnect between nanotubes within the ABS matrix on modification. With addition of 1 and 5 phr high density polyethylene, Wu et al.²⁸ found that the percolation threshold of polymethyl methacrylate/carbon nanofiber composite was reduced from 8.0 to 4.0 phr. In our present work, LCP was added to the ABS/MWCNTs composite with the idea that LCP composites more readily form an interconnected conducting network than other thermoplastics, as reported by Lozano et al.²⁹ A significant decrease in resistivity was observed with addition of 15 phr LCP to ABS/MWCNTs (1.5 phr, modified MWCNTs) composite (2.2×10^4). FESEM confirms the high degree of dispersion with distinguishable nanotubes within the ABS matrix with the addition of LCP to ABS/MWCNTs composite containing 1.5 phr of modified CNTs.

CONCLUSIONS

ABS/CNT composites were prepared successfully by melt blending ABS, CNT, and LCP. The properties of composites were investigated using FESEM, DSC, and DMTA. From FESEM images, it was observed that strong interaction exists between ABS and acid-modified MWCNTs' this leads to effective stress transfer at the interface between MWCNTs and matrix polymer (ABS) that is evident in the large increase in mechanical properties. Formation of network structure has been observed in modified MWCNTs composites. The storage modulus (E') and glass transition temperature (T_g) of the matrix polymer (ABS) is significantly increased, particularly with the addition of modified MWCNTs. The electrical resistivity of MWCNTs composites decreased as compared to pure ABS. The reduction was more for modified composites due to formation of a network structure at same amount of MWCNTs. Addition of LCP to ABS/MWCNTs (modified) composite resulted in further increase in thermal and electrical properties due to the formation of interface and additional bond between MWCNTs and acrylic elastomer.

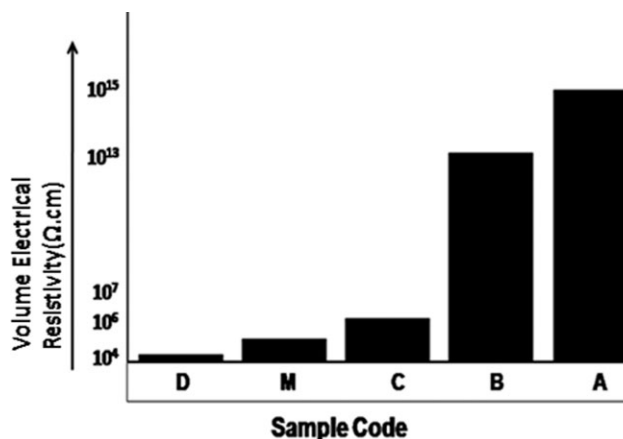


Figure 6. Volume electrical resistivity of the nanocomposites.

ACKNOWLEDGEMENT

The authors specially thank UGC New Delhi, India, for granting the kind financial support for the research work.

REFERENCES

1. Wang, D.; Li, Y.; Xie, X. M.; Guo, H. B. *Polymer* **2011**, *52*, 191.
2. Mohammadi, M.; Yousefi, A. A.; Ehsani, M. J. *Appl. Polym. Sci* **2012**, *125*, 755.
3. Kudva, R. A.; Keskkula, H.; Paul, D. R. *Polymer* **1998**, *39*, 2447.
4. Lahelin, M.; Annala, M.; Nykänen, A.; Ruokolainen, J.; Seppälä, J. *Compos. Sci. Technol.* **2011**, *71*, 900.
5. Park, S. H.; Thielemann, P.; Asbeck, P.; Bandaru, P. R. *Appl. Phys. Lett.* **2009**, *94*, 243111.
6. Balberg, I. *Phys. Rev. B* **1985**, *31*, 4053.
7. Bauhofer, W.; Kovacs, J. Z. *Compos. Sci. Technol.* **2009**, *69*, 1486.
8. Kara, S.; Arda, E.; Dolastir, F.; Pekcan, O. J. *Colloid. Interf. Sci.* **2010**, *344*, 395.
9. Thorstenson, E. T.; Ren, Z.; Chou, T. W. *Compos. Sci. Technol.* **2001**, *61*, 1899.
10. Jang, J.; Bae, J.; Yoon, S. H. *J. Mater. Chem.* **2003**, *13*, 676.
11. Viswanathan, G.; Chakrapani, N.; Yang, H.; Wei, B.; Chung, H.; Cho, K. J. *Am. Chem. Soc.* **2003**, *125*, 9258.
12. Ree, M.; Kim, K.; Woo, S. H.; Chang, H. J. *Appl. Phys.* **1997**, *81*, 698.
13. Meincke, O.; Kaempfer, D.; Weickmann, H.; Friedrich, C.; Vathauer, M.; Warth, H. *Polymer* **2004**, *45*, 739.
14. Potschke, P.; Bhattacharaya, A. R. *Polym. Prepr.* **2003**, *44*, 760.
15. Jurewicz, I.; Worajittiphon, P.; King, A. A. K.; Sellin, P. J.; Keddie, J. L.; Dalton, A. B. *J. Phys. Chem. B* **2011**, *115*, 6395.
16. Bose, S.; Mukherjee, M.; Das, C. K.; Saxena, A. K. *J. Nano-sci. Nanotechnol.* **2009**, *9*, 1.
17. Needleman, A.; Borders, T. L.; Brinson, L. C.; Flores, V. M.; Schadler, S. *Compos. Sci. Technol.* **2010**, *70*, 2207.
18. Nayak, G. C.; Rajasekar, R.; Das, C. K. *J. Mater. Sci.* **2011**, *46*, 2050.
19. Jung, Y. C.; Sahoo, N. G.; Cho, J. W. *Macromol. Rapid Commun.* **2006**, *27*, 126.
20. Xu, J.; Chatterjee, S.; Koelling, K. W.; Wang, Y.; Becthel, S. E. *Rheol. Acta* **2005**, *44*, 537.
21. Bose, S.; Pramanik, N.; Das, C. K.; Ranjan, A.; Saxena, A. K. *Mater. Des.* **2010**, *31*, 1148.
22. Nayak, G. C.; Rajasekar, R.; Das, C. K. *J. Appl. Polym. Sci.* **2011**, *119*, 3574.
23. Hatui, G.; Sahoo, S.; Das, C. K.; Saxena, A. K.; Basu, T.; Yue, C. Y. *Mater. Des.* **2012**, *42*, 184.
24. Ma, P. C.; Kim, J. K.; Tang, B. Z. *Carbon* **2006**, *44*, 3232.
25. Bose, S.; Mukherjee, M.; Pal, K.; Nayak, G. C.; Das, C. K. *Polym. Adv. Technol.* **2010**, *21*, 272.
26. Blom, H.; Yeh, R.; Wojnarowski, R.; Ling, M. *Thermochim. Acta* **2006**, *442*, 64.
27. Mukherjee, M.; Das, T.; Rajasekar, R.; Bose, S.; Das, C. K. *Compos. Appl. Sci. Manuf.* **2009**, *40*, 1291.
28. Wu, G.; Asai, S.; Sumita, M. A. *Macromolecules* **1999**, *32*, 3534.
29. Lozano, K.; Bonilla-Rois, J.; Barrera, E. V. *J. Appl. Polym. Sci.* **2001**, *80*, 1162.